Available online at www.sciencedirect.com

SciVerse ScienceDirect

Advances in Space Research 49 (2012) 185–195

ADVANCES IN SPACE RESEARCH (a COSPAR publication)

www.elsevier.com/locate/asr

Earth and Mars observation using periodic orbits

E. Ortore [a,*], C. Circi [b], F. Bunkheila [a], C. Ulivieri [a]

[a] Centro di Ricerca Progetto S. Marco (CRPSM), Sapienza University of Rome, Via Salaria, 851, 00138 Rome, Italy
[b] Department of Astronautics, Electrics and Energetic Engineering, Sapienza University of Rome, Via Salaria, 881, 00138 Rome, Italy

Received 16 June 2011; received in revised form 15 September 2011; accepted 16 September 2011
Available online 21 September 2011

Abstract

This paper reports the results of a general study carried out on the Periodic Multi-SunSynchronous Orbits (PMSSOs), which the classical Periodic SunSynchronous Orbits (PSSOs) represent a specific solution of. Such orbits allow to obtain cycles of observation of the same region in which the solar illumination regularly varies according to the value of the orbit elements and comes back to the initial condition after a time interval which is multiple of the revisit time. Therefore this kind of orbits meets all the remote sensing applications that need observations of the same area at different local times (for example the reconstruction of the day-nighttime trend of the surface temperature of the planet) and it is particularly suitable to the study of several terrestrial and martian phenomena (diurnal cycle of the hazes and clouds, dynamics of the thermal tides, density variations, meteorology phenomena, etc.). The design of PMSSO is based on the variation of the Right Ascension of the Ascending Node due to the Earth oblateness (referred as basic solution). However, with respect to the basic solution, the analysis of the perturbative effects has demonstrated the need, especially in the case of Mars, to take into account all the superior harmonics of the gravitational field. To this end a corrective factor, to add to the basic equations, has been proposed, allowing a significant saving of propellant (of the order of 2 km/s per year). Besides, single and multi-plane satellite constellations have been taken into account in order to improve the repetition of observation and the ground spatial resolution.
© 2011 COSPAR. Published by Elsevier Ltd. All rights reserved.

Keywords: Multi-SunSynchronous Orbits; Mars orbits; Gravitational perturbations

1. Introduction

The requirements of a planetary observation system are strictly related to the orbit design and, in particular, to its shape and inclination. In regards to the observation of the Earth, the ground resolution, the coverage (both in latitude and in longitude), the repetition of observation, the same condition of solar illumination, often lead to consider the Periodic SunSynchronous Orbits (PSSOs) as the most suitable ones. In fact, these orbits allow to observe a given region of the planet at regular time intervals (periodic orbits) with approximately the same solar illumination conditions (SunSynchronism). Unlike the strict SunSynchronous Orbits (SSOs), which are characterized by a typical relationship between orbit altitude and inclination and that can be opportunely modified using solar sail systems (Bolle and Circi, 2011), the introduction of the periodicity (repetition of observation) limits the possible altitudes to a finite number (represented by the points belonging to the aforesaid altitude–inclination curve). The choice of the solution results from a compromise among the several requirements since it is not possible to have the best solution for all of them (e.g. the coverage and the repetition of observation are in contrast).

The Periodic Multi-SunSynchronous Orbits (PMSSOs), which the classical PSSOs are a particular solution of, represent an important alternative to the use of the PSSOs. The PMSSOs form a general category of orbits that are characterized by two periodicity conditions: the first is related to the observation of a given area (periodic orbit), the second one refers to the solar illumination, which repeats itself at

* Corresponding author.
E-mail addresses: ortore@psm.uniroma1.it (E. Ortore), christian.circi@uniroma1.it (C. Circi), fbunkheila@gmail.com (F. Bunkheila), ulivieri@psm.uniroma1.it (C. Ulivieri).

0273-1177/$36.00 © 2011 COSPAR. Published by Elsevier Ltd. All rights reserved.
doi:10.1016/j.asr.2011.09.016

regular time intervals (Multi-SunSynchronism). The two periodicities are properly linked so as to obtain cycles of observation of the same area in which the solar illumination gradually varies along with the choice of the orbit elements and returns to the initial condition after a number of nodal days which is multiple of the revisit time. A significant advantage of the PMSSOs lies in the great flexibility as far as choice of the orbit inclination is concerned (the SSOs are retrograde and usually quasi-polar and for that matter a limitation of the exploitable launching sites is determined) (Ulivieri and Anselmo, 1991).

In this paper, with reference to circular orbits, the feasibility of employing the Multi-SunSynchronous technique is investigated in depth, with reference to both Earth and Mars observation. Furthermore, a selection was carried out to find the most suitable solutions in terms of orbit altitude and inclination, as well as of repetition cycles on observation frequency and solar illumination conditions.

The PMSSO solution represents an innovative element for all those applications that can get advantage of data analysis deriving from measurements carried out on the same area but with different solar illumination conditions (e.g. reconstruction of the day-nighttime trend of the surface temperature of the planet). In particular, the use of the PMSSOs on Mars should allow for an estimate of several atmospheric phenomena. In fact, since the diurnal variations of several martian atmospheric phenomena are very wide (diurnal cycle of the hazes and clouds, dynamics of the thermal tides, density variations, meteorology phenomena, etc.) the observations should extend over a complete sol (martian day) Hess et al., 1979; Cantor et al., 2002; Tamppari et al., 2003; Goody and Belton, 1967; Paige and Wood, 1992. Therefore, while PSSOs are not suitable for the study these martian phenomena (Capderou and Forget, 2004), on the other hand the PMSSOs, thanks to the possibility of performing a complete sol sampling, find their most appropriate employment. In particular, the observation of the martian polar regions at various local times is of key importance in order to study the water cycle (northern polar cap source), the CO_2 cycle (polar caps), the dust cycle (cap edge dust storms), and the atmospheric dynamics (high latitude baroclinic waves, polar warming, etc.).

2. Periodic Multi-SunSynchronous Orbits

The equations identifying a PMSSO are the following:

$$m \cdot D_n = R \cdot T_n \tag{1}$$

$$n \cdot D_n = \frac{2\pi}{|\dot{\Omega}_S - \dot{\Omega}|} \tag{2}$$

$$n = I \cdot m \tag{3}$$

Eq. (1) represents the condition of periodicity on the observation of the same area: the satellite performs the same ground tracks at regular temporal intervals (periodic orbit). Taking into account the perturbative effects, a periodic orbit is obtained whilst within a certain time interval, called revisit time and measured in an integer number m of nodal days D_n, the satellite describes an integer number R of nodal periods T_n (Kalil and Martikan, 1963). Every m nodal days (or R nodal periods; R and m are prime to one another) the sub-satellite point comes back on the same point of the surface of the planet thus allowing the observation of the same area. The expressions of the nodal day (time necessary for a point on the equator of the planet to re-encounter the nodal line of satellite orbit) and of the nodal period (temporal interval between consecutive passages of satellite at the ascending node) are the following:

$$D_n = \frac{2\pi}{\omega_P - \dot{\Omega}} \tag{4}$$

$$T_n = \frac{2\pi}{\dot{\xi}} \tag{5}$$

where $\dot{\xi} = \dot{\omega} + \dot{M}$ ($\xi = \omega + M =$ argument of latitude, $\dot{M} = \sqrt{\frac{\mu_P}{a^3}} + \dot{M}_{Pert}$ with $\mu_P =$ gravitational constant of the planet and $a =$ semi-major axis of the orbit), $\dot{\Omega}$, $\dot{\omega}$, $\dot{M}_{Pert}$ are respectively the temporal variations of the Right Ascension of the Ascending Node (RAAN $= \Omega$), the argument of perigee ω and the mean anomaly M of the satellite due to the perturbative effects; ω_P is the rotation angular velocity of the planet around its axis. Since we consider circular PMSSOs, ω and M are not singularly defined and the angular position of the satellite is calculated with respect to the ascending node by means of the parameter ξ.

Eq. (2) allows to observe the same latitudes, but in general at a different longitude, at the same local time every n nodal days (condition of Multi-SunSynchronism with the Sun; n is an integer number); $\dot{\Omega}_S$ is the Sun angular velocity in the apparent motion with respect to the planet. The particular case of SSO corresponds to the mathematical condition $n \to \infty$ ($\dot{\Omega} = \dot{\Omega}_S$); in this case the nodal day is equal to the solar day of the planet.

Eq. (3), where I is an integer number, links the conditions (1) and (2); since n is a multiple of the revisit time m, the satellite observes each zone I times in n nodal days, and every time at a different local time.

Fig. 1 shows a schematisation of the angular displacements, in the equatorial plane, of the Sun, planet and line of nodes; whenever the orbital plane re-encounters the Sun (it occurs every n nodal days), the same illumination conditions occur again (Multi-SunSynchronism); r is the radius of the orbit and i is the orbit inclination.

2.1. Perturbative effects on Earth and Mars PMSSOs

The characteristics of the Earth and Mars allow the realization of the Multi-SunSynchronism since the zonal harmonic J_2 (due to the planet oblateness, which is equal to 1.0822×10^{-3} and 1.955454×10^{-3} for Earth and Mars, respectively) represents the predominant perturbative gravitational term, while the solar radiation pressure and third-body perturbation, both for Earth and Mars orbits

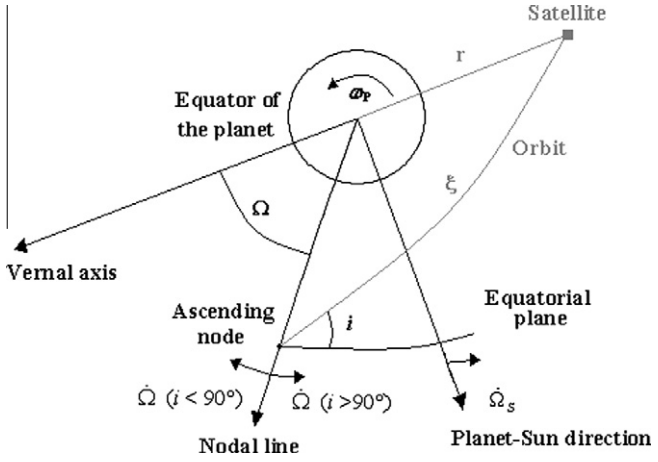

Fig. 1. Angular displacements of the Sun, planet and nodal line.

up to an altitude $h = 10{,}000$ km (for circular orbits), do not imply significant effects. As for the atmospheric drag, for low Earth and Mars orbits it is necessary to carry out appropriate corrective manoeuvres of altitude re-positioning to control the consequent eastward ground track drift.

However, an accurate analysis on the perturbative gravitational effects of both Earth and Mars has led to the conclusion that, for low-altitude orbits, in order to gain a very precise PMSSO solution, it is not possible to completely neglect the effects due to the superior harmonics. Therefore, the consideration of the only J_2 can be seen as a PMSSO basic solution and the introduction of an appropriate corrective factor depending on the orbit altitude and its inclination, will allow to obtain the precise PMSSO solution (see Section 5).

2.2. Periodicity condition

For a circular orbit, the variations of RAAN and of the argument of latitude (ξ) due to the effect of J_2 may be expressed by the following well-known expressions:

$$\dot{\Omega}_{J2}(r,i) = -\frac{K_2 \cdot \cos i}{r^{7/2}} \tag{6}$$

$$\dot{\xi}_{J2}(r,i) = \dot{\omega}_{J2} + \dot{M}_{J2} = \frac{K_2 \cdot (4\cos^2 i - 1)}{r^{7/2}} \tag{7}$$

where $K_2 = \frac{3}{2} J_2 R_P^2 \sqrt{\mu_P}$ and R_P is the mean equatorial radius of the planet. By replacing Eqs. (6) and (7) in (4) and (5) and then considering the following approximated expression for the nodal period (Ulivieri and Anselmo, 1991):

$$T_n \cong 2\pi \sqrt{\frac{r^3}{\mu_P}} \left[1 - \frac{K_2 (4\cos^2 i - 1)}{r^2 \sqrt{\mu_P}} \right] \tag{8}$$

it is possible to reduce the periodicity condition (1) to the solution of the following polynomial equation:

$$a_1 \cdot r^{5.5} + a_2 \cdot r^4 + a_3 \cdot r^{3.5} + a_4 \cdot r^2 + a_5 = 0 \tag{9}$$

in which the unknown variable is the radius of the circular orbit and some coefficients depend on i, m and R:

$$a_1 = \frac{\omega_P}{\sqrt{\mu_P}}$$

$$a_2 = -\frac{m}{R}$$

$$a_3 = -\frac{K_2 \omega_P (4\cos^2 i - 1)}{\mu_P}$$

$$a_4 = \frac{K_2 \cos i}{\sqrt{\mu_P}}$$

$$a_5 = -\frac{K_2^2 \cos i (4\cos^2 i - 1)}{\mu_P}$$

For assigned values of i, m, R (note that m and R are linked by Eq. (1)) the physically acceptable solutions of Eq. (9) provide the values of the radius of the corresponding periodic orbits. In fact, only a discrete number of values of r satisfies Eq. (9).

In the cases of Mars and the Earth, Figs. 2 and 3 show respectively the temporal variations of $\dot{\Omega}_{J2}$ and $\dot{\xi}_{J2}$ (in deg/day) as a function of the inclination (Eqs. (6) and (7)).

As evidence shows, the orbits of Mars present higher variations with respect to the ones of the Earth, especially for low inclination values. This peculiarity, together with the different values of $\dot{\Omega}_S$ and ω_P, leads to a shift of the martian altitude–inclination curve for the SSOs (based on the condition $\dot{\Omega}_{J2} = \dot{\Omega}_S$), to different values of the nodal day (Eq. (4) and nodal period (Eq. (5) and therefore to different orbit periodic solutions (Eq. (1)), and to a different condition of Multi-SunSynchronism with the Sun (Eq. (2).

2.3. PMSSO basic solution

Replacing Eq. (6) in (4) and then in (2), mathematical calculations produce the condition of multi-synchronism with the Sun in the following form (– for $\dot{\Omega}_{J2} < \dot{\Omega}_S$, + for $\dot{\Omega}_{J2} > \dot{\Omega}_S$):

$$r^{3.5} = -K_2 \frac{n \mp 1}{n\dot{\Omega}_S \mp \omega_P} \cos i \tag{10}$$

Moreover, by retrieving the term "$\cos i$" by Eq. (10) and replacing it in (9) (coefficients a_3, a_4, a_5), it follows that:

$$b_1 \cdot r^7 + b_2 \cdot r^2 + b_3 \cdot r^{0.5} + b_4 = 0 \tag{11}$$

where

$$b_1 = \frac{4}{\mu_P K_2} \cdot \left(\frac{n\dot{\Omega}_S \pm \omega_P}{n \pm 1} \right)^2$$

$$b_2 = -\frac{1}{\sqrt{\mu_P}}$$

$$b_3 = -\frac{m}{R} \cdot \frac{n \pm 1}{n \cdot (\dot{\Omega}_S - \omega_P)}$$

$$b_4 = -\frac{K_2}{\mu_P}$$

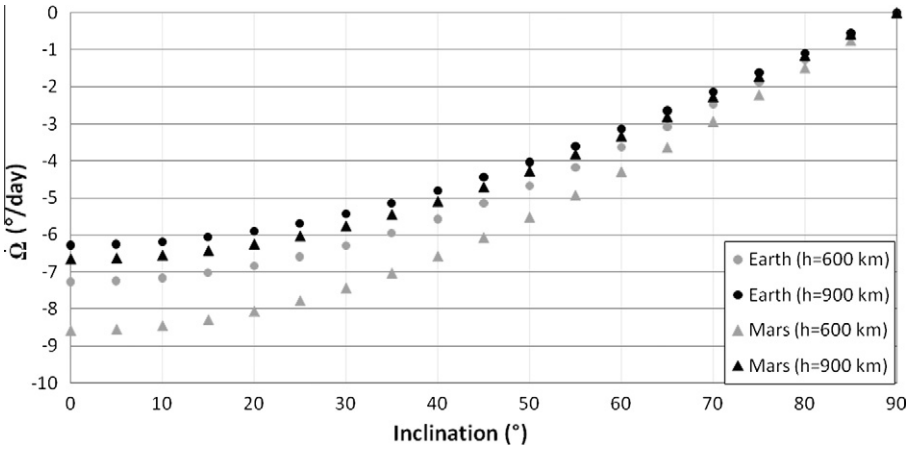

Fig. 2. Earth and Mars: temporal variation of $\dot{\Omega}_{J2}$ as a function of i.

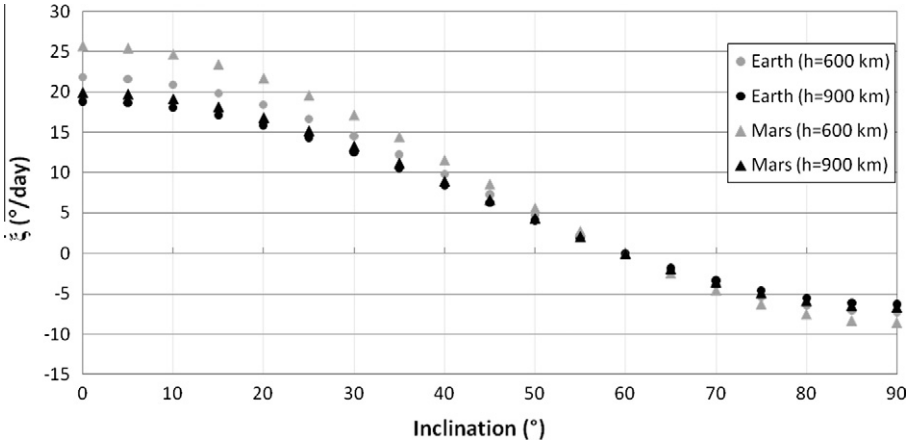

Fig. 3. Earth and Mars: temporal variation of $\dot{\xi}_{J2}$ as a function of i.

Once the values of n, m (or I, according to the condition (3)) and R are fixed, the solution of Eq. (11) provides the radius of a PMSSO. The corresponding inclination value can be obtained by solving Eq. (10). If on one hand the solutions of Eq. (10) are theoretically infinite, there are only a discrete number of PMSSO solutions (Eq. (11)).

Considering Eq. (4), (2) becomes:

$$n = \frac{\omega_P - \dot{\Omega}}{|\dot{\Omega}_S - \dot{\Omega}|} \tag{12}$$

Since both for the Earth and Mars $\omega_P \gg \dot{\Omega}$, low values of n cannot be obtained (the lower limit of n depends on h and i).

2.4. Satellite ground track pattern

Ground track analysis plays a key role in the mission design. In fact, the minimum distance between ground tracks at the end of the revisit time m is directly linked both to the possibility to gain a complete longitudinal coverage of the planet and to the ground spatial resolution. The westward longitudinal separation (S_t) between successive equatorial crossings of the sub-satellite point (successive passages at the ascending node) is given by:

$$S_t = T_n(\omega_P - \dot{\Omega}) \cdot R_P = \frac{2\pi R_P}{q} \tag{13}$$

where q is the number of orbits performed by the satellite each day (repetition factor). At the end of the revisit time, the equatorial ground track spacing (S_m) is:

$$S_m = \frac{S_t}{m} \tag{14}$$

Therefore, for a full longitudinal coverage of the surface of the planet (the ground tracks become closer one to the other as the latitude increases), the swath width L of the instruments, considering the cross-track direction, has to satisfy the condition:

$$L \geqslant S_m \cdot \sin i = \frac{S_t}{m} \cdot \sin i = \frac{2\pi R_P \cdot \sin i}{R} \tag{15}$$

However, when the swath width L (and S_m) increases (it is inversely correlated to the value of m, according to Eq. (15)), the ground spatial resolution that can be obtained by a given instrument degrades. On the contrary, reducing

S_m, the ground spatial resolution improves but the same area is observed after a greater number of nodal day m (degradation of the repetition of observation). Therefore, the choice of the orbit elements has to be based on a compromise between the two (antithetical) mission requirements: revisit time and spatial resolution; it depends on the particular goal of the mission (frequency of observation and observational detail required to investigate a given phenomenon).

The repetition factor can be written as:

$$q = \frac{R}{m} = N_i + N_f = N_i + \frac{k}{m} \tag{16}$$

where N_i is the number of integer orbits performed by the satellite each day and N_f the fractional part. When q is not an integer number, N_f is composed by two integers prime to one another, k and m (with $1 \leqslant k \leqslant m-1$; R and m also are prime to one another). The parameter k, depending on the altitude of the satellites, is related to the way the ground tracks are repeated. In fact, the $m-1$ ground tracks of the orbits subsequent to the N_ith will fall inside the interval S_t and in m days the subdivision of S_t in m intervals S_m will occur. Indicating with S_d the daily displacement of the ground tracks, which represents the distance at the equator between tracks related to subsequent days, it follows that:

$$S_d = -S_m \cdot k \text{ for } k \leqslant \frac{m}{2}, \quad S_d = S_m(m-k) \text{ for } k > \frac{m}{2} \tag{17}$$

The daily ground track displacement is direct eastward ($S_d < 0$) for $k < m/2$, westward ($S_d > 0$) for $k > m/2$ ($k = m/2$ can be obtained only in the case $k = 1$, $m = 2$); in particular, $S_d = -S_m$ for $k = 1$ and $S_d = S_m$ for $k = m-1$. If q is an integer value, then $m = 1$ ($k = 0$).

3. Basic solution for the Earth

Considering only J_2 both in the periodicity (1) and in Multi-SunSynchronism (2) conditions led to obtain Eq. (10), and therefore to determine all the PMSSO solutions. However, such a relationship, which neglects superior harmonics of gravitational field, provides a basic solution, improvable with the introduction of an appropriate corrective factor.

Fig. 4 reports some solutions (for different values of n) of Eq. (10) for the Earth; in this case: $\omega_P = 7.29212 \times 10^{-5}$ rad/s, $\dot{\Omega}_S = 1.99102 \times 10^{-7}$ rad/s, $\mu_P = 398600.44$ km^3/s^2 and $R_P = 6378.135$ km.

As evidence shows, for direct orbits, the value of n for a given orbit altitude decreases along with the inclination. For retrograde orbits this trend is inverted and the values of n are higher. The optimal range of application of this kind of orbit for Earth observation is the one related to the observation of mid-low latitudes (low values of h, i, n).

Fig. 5 shows the 8 PMSSO solutions (discrete values of h are obtained by Eq. (11) and the corresponding value of i by Eq. (10)), for the following values of h, i and m:

$$\begin{cases} 600 \leqslant h \leqslant 900 \text{ km} \\ 24 \leqslant i \leqslant 36^\circ \\ 3 \leqslant m \leqslant 5 \end{cases}$$

While a low altitude allows to obtain a good spatial resolution and a low inclination optimises the observation of low latitudes, the selected m-interval provides a good compromise between revisit time and spatial resolution.

The n values allow to carry out cycles of observation ranging from 50 to 56 nodal days. While the investigation of measurements related to a single cycle may allow to evaluate the 24-h trends (short-term variations) of terrestrial and atmospheric parameters and phenomena, the study of the differences between a cycle and another may allow the estimation of their seasonal and annual variations (long-term variations). For example, with the orbit corresponding to point B, since a given region is observed every $m = 3$ nodal days and the same local time is re-obtained every $n = 54$ nodal days, the region is observed, at regular time intervals, in $I = n/m = 18$ different illumination conditions.

The characteristic parameters of the 8 solutions A–H (Fig. 5) are reported in Table 1.

3.1. The use of satellite constellations

If the parameters S_m and m for a single satellite do not guarantee the required coverage and/or the required repetition, it is necessary to resort to a constellation. In fact, unlike in the case of a single satellite, the use of satellite constellations can be addressed either to increase the repetition of observation (satellites perform the same ground track at different times) or to reduce the minimum spacing between ground tracks in order to limit the sensor swath size needed to achieve a complete longitudinal coverage of the surface (satellites perform different ground tracks to thicken the pattern: improvement of the ground spatial resolution).

In particular, a repetition of observation of less than one nodal day is achievable only when different orbital planes are taken into account (a revisit frequency inferior to one nodal day cannot be achieved both for single satellite and for single plane; in fact m is an integer number of nodal days).

The orbits taken into account have the same r, i, k, m and n values (uniform constellations).

3.1.1. Single-plane constellations

In case of a single-plane, considering orbits with the same values of radius, inclination, k, m and n (uniform constellations), the relationship that must be satisfied for the satellites to perform the same ground track is (Hopkins, 1988):

$$\Delta M_i = 2\pi\left(1 - \frac{k}{m}\right) \cdot d \tag{18}$$

where ΔM_i is the relative inter-orbit phasing between the satellite i and 1 and d is the integer number of nodal days

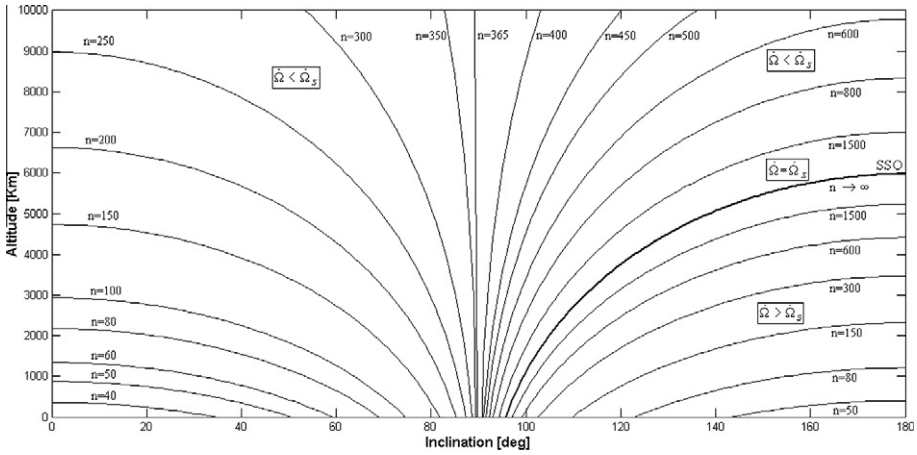

Fig. 4. Solution of Eq. (10) for the Earth.

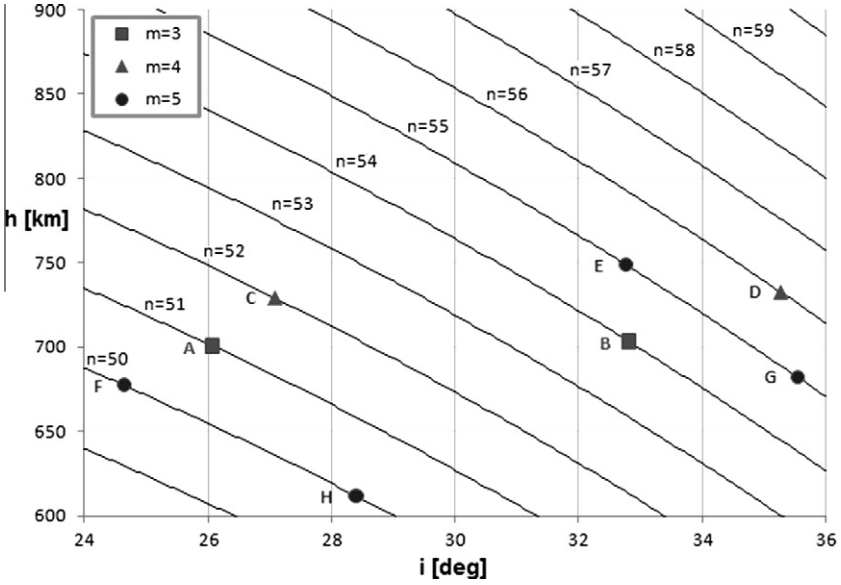

Fig. 5. Low and direct PMSSOs for the observation of tropical regions.

Table 1
Parameters related to the PMSSO solutions of Fig. 5.

	m	n	k	R	q	h (km)	i (°)	S_m (km)
A	3	51	1	43	14 + 1/3	700.58	26.09	931.98
B	3	54	1	43	14 + 1/3	703.3	32.82	931.98
C	4	52	1	57	14 + 1/4	729.51	27.08	703.08
D	4	56	1	57	14 + 1/4	733	35.27	703.07
E	5	55	1	71	14 + 1/5	749.08	32.76	564.42
F	5	50	2	72	14 + 2/5	677.42	24.64	556.58
G	5	55	2	72	14 + 2/5	682	35.56	556.58
H	5	50	3	73	14 + 3/5	611.78	28.39	548.95

between two observations over the same track. Therefore, when the first satellite is in place, by considering other $N_S - 1$ satellites which satisfy Eq. (18) (with, respectively $d = 1, \ldots, N_S - 1$; $N_S =$ total number of satellites), a fixed region is surveyed N_S times in m nodal days ($N_S \leqslant m$) while the ground track spacing is equal to that of a single satellite.

In order to obtain a daily observation frequency (with reference to the nodal days) it is therefore necessary to consider a number of satellites $N_S = m$. Since an observation frequency inferior to one nodal day cannot be achieved with satellites orbiting on the same orbital plane, it is meaningless to consider a number of satellites $N_S > m$ (in fact, referring to

Eq. (18), the position of the $(N_S + 1)$ satellite matches with the one of satellite 1, the position of the $(N_S + 2)$ satellite coincides with the one of satellite 2, and so on). With $N_S = m$ the satellites result evenly shifted in mean anomaly one to another (the shift is equal to $360°/N_S$).

For example, considering orbit B of Table 1, it is possible to create a 3-satellite ($N_S = m = 3$) single-plane PMSSO constellation, which guarantees a daily Earth observation; according to Eq. (18), the satellites must be shifted in mean anomaly of 120° one to another. The corresponding local times at the ascending node during $n = 54$ nodal days are reported in Table 2 (starting at 10:00 on September 1st, 2010). As evidence shows, the satellites allow an observation of the same region at regular time intervals of $D_n = 23\text{ h }33'20''$.

An important example of application on the use of PMSSO constellations is represented by the reconstruction of the 24-h trend of the surface temperature of the Earth. Using a passive satellite sensor, appropriate measurements in the atmospheric windows (intervals of the electromagnetic spectrum in which the interaction between radiation and atmosphere is minimized) of the Thermal Infrared Region (TIR) (between 10 and 12 μm) allow to calculate the brightness temperature of the Earth. Taking into account the correction of the atmospheric absorption and the surface emissivity effect using the General Split Window Technique (GSWT), Ulivieri et al. (1994), the 24-h surface temperature trend can be accurately estimated.

Fig. 6 shows the possible reconstruction of the diurnal variation of the surface temperature of the Earth that can be obtained using the three-satellite constellation B. With a constellation of three satellites in PSSO it should be possible to have only three different measurements.

3.1.2. Multi-plane constellations

The addition of one or more orbital planes (evenly shifted in RAAN) can be taken into consideration either to further increase the observation frequency (making the satellites perform the same ground tracks) or the spatial resolution (by reducing the minimum ground track spacing S_m with respect to the case of single plane). Calling P the number of orbital planes and with $lcm(m, N_{SP})$ the least common multiple between m and N_{SP}, where N_{SP} is the number of satellites for each plane (same number for each plane), the minimum temporal interval of revisit Δt (in nodal days) obtainable on the same area and the minimum ground track spacing $S_{\min}$ (in km) are given by $\Delta t = \frac{lcm(m,N_{SP})}{P \cdot N_{SP}}$ and $S_{\min} = \frac{S_t}{P \cdot lcm(m,N_{SP})}$. For $P = 1$ ($N_{SP} = N_S$) the single-plane constellation case is obtained.

As evidence shows, the value of Δt is not necessarily an integer number of nodal days (like in the single-plane case) and it is possible to obtain a revisit interval inferior to one nodal day; in this case it is mandatory to increase in the number of satellites with respect to the case $P = 1$. In order to obtain an interval of revisit that is constant and equal to Δt it is necessary to consider a number of satellite for each

Table 2
Ascending node local time for the three-satellite constellation of case B.

Nodal days	Satellite	Solar days	Local time	Nodal days	Satellite	Solar days	Local time
0	1	01 Sep	10.00:00	27	1	27 Sep	22:00:00
1	2	02 Sep	09:33:20	28	2	28 Sep	21:33:20
2	3	03 Sep	09:06:40	29	3	29 Sep	21:06:40
3	1	04 Sep	08:40:00	30	1	30 Sep	20:40:00
4	2	05 Sep	08:13:20	31	2	01 Oct	20:13:20
5	3	06 Sep	07:46:40	32	3	02 Oct	19:46:40
6	1	07 Sep	07:20:00	33	1	03 Oct	19:20:00
7	2	08 Sep	06:53:20	34	2	04 Oct	18:53:20
8	3	09 Sep	06:26:40	35	3	05 Oct	18:26:40
9	1	10 Sep	06:00:00	36	1	06 Oct	18:00:00
10	2	11 Sep	05:33:20	37	2	07 Oct	17:33:20
11	3	12 Sep	05:06:40	38	3	08 Oct	17:06:40
12	1	13 Sep	04:40:00	39	1	09 Oct	16:40:00
13	2	14 Sep	04:13:20	40	2	10 Oct	16:13:20
14	3	15 Sep	03:46:40	41	3	11 Oct	15:46:40
15	1	16 Sep	03:20:00	42	1	12 Oct	15:20:00
16	2	17 Sep	02:53:20	43	2	13 Oct	14:53:20
17	3	18 Sep	02:26:40	44	3	14 Oct	14:26:40
18	1	19 Sep	02:00:00	45	1	15 Oct	14:00:00
19	2	20 Sep	01:33:20	46	2	16 Oct	13:33:20
20	3	21 Sep	01:06:40	47	3	17 Oct	13:06:40
21	1	22 Sep	00:40:00	48	1	18 Oct	12:40:00
22	2	23 Sep	00:13:20	49	2	19 Oct	12:13:20
23	3	23 Sep	23:46:40	50	3	20 Oct	11:46:40
24	1	24 Sep	23:20:00	51	1	21 Oct	11:20:00
25	2	25 Sep	22:53:20	52	2	22 Oct	10:53:20
26	3	26 Sep	22:26:40	53	3	23 Oct	10:26:40
				54	1	24 Oct	10:00:00

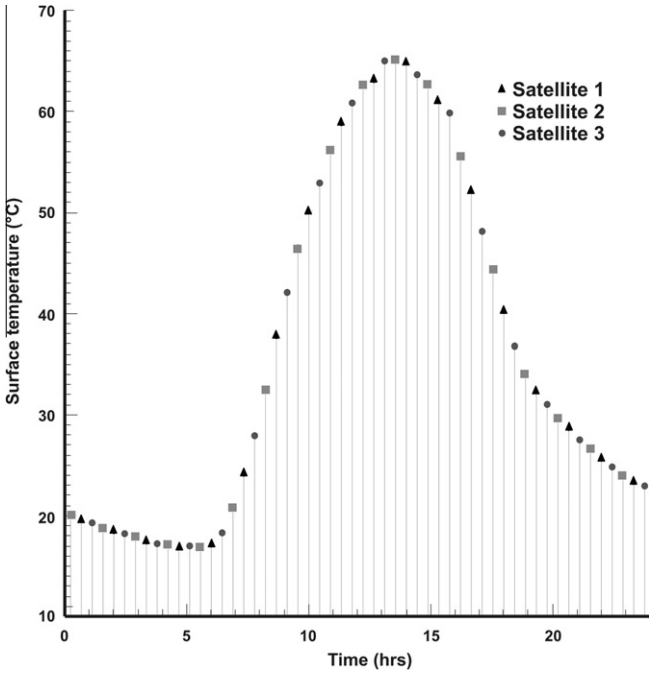

Fig. 6. Example of surface temperature reconstruction by using the constellation of Table 2.

plane $N_{SP} = m$; in this case $\Delta t = 1/P$ nodal days (the satellites of each plane must satisfy Eq. (18) and the orbital planes must be opportunely shifted in RAAN).

4. Basic solution for Mars

Similarly to the case of the Earth, Fig. 7 reports some PMSSO solutions for Mars; in this case: $\omega_P = 7.08822 \times 10^{-5}$ rad/s, $\dot{\Omega}_S = 1.03026 \times 10^{-7}$ rad/s, $\mu_P = 4.2828372 \times 10^4$ km^3/s^2 and $R_P = 3396.2$ km. In general the value of n increases more rapidly than for the Earth.

For Mars, two regions of interest have been selected. The first one (that is useful for the study of the diurnal cycle of the hazes and clouds, dynamics of the thermal tides, density variations, meteorological phenomena, etc.) refers to the mid-low latitudes. The second one (suitable for the study of the water cycle, the CO_2 cycle, the dust cycle and the atmospheric dynamic) refers to high latitude observations.

Fig. 8 (mid-low latitude observations) shows the 10 possible PMSSO solutions for:

$$\begin{cases} 700 \leqslant h \leqslant 900 \text{ km} \\ 24 \leqslant i \leqslant 36^\circ \\ 3 \leqslant m \leqslant 5 \end{cases}$$

The n values allow to carry out cycles of observation going from 50 to 57 nodal days.

Fig. 9 (high latitude observations) shows the 16 possible PMSSO solutions for:

$$\begin{cases} 700 \leqslant h \leqslant 900 \text{ km} \\ 77 \leqslant i \leqslant 78^\circ \\ 3 \leqslant m \leqslant 5 \end{cases}$$

In this case the values of n are significantly higher in comparison to the ones of Fig. 8 (longer observation cycles).

The characteristic parameters of some solutions of Figs. 8 and 9 are reported in Table 3. The values obtained for S_m allow a ground spatial resolution that is considerably higher than the one achievable on the Earth (Table 1).

5. The complete solution

As previously mentioned, to obtain a precise PMSSO solution, it is mandatory to take into account the effects due to the superior harmonics. In order to carry out a complete evaluation of all the gravitational effects, several numerical simulations were carried out using "complete models" of (21 × 21) (order and degree) and (40 × 40) harmonics for the Earth and Mars, respectively. The numerical values of the harmonics used in such simulations are the EGM96 (Earth Gravity Model 96), Lemoine et al. (1998), and GMM-2B (Goddard Mars Model 2B), Lemoine et al. (2001), for the Earth and Mars, respectively (URL: http://cddis.nasa.gov/926/egm96/egm96.html; http://denali.gsfc.nasa.gov/697/MARS/GMM2B.html). The equations of motion were propagated both in the case "Keplerian plus J_2" and "complete models" and, after 1 year of propagation, the difference in the value of RAAN

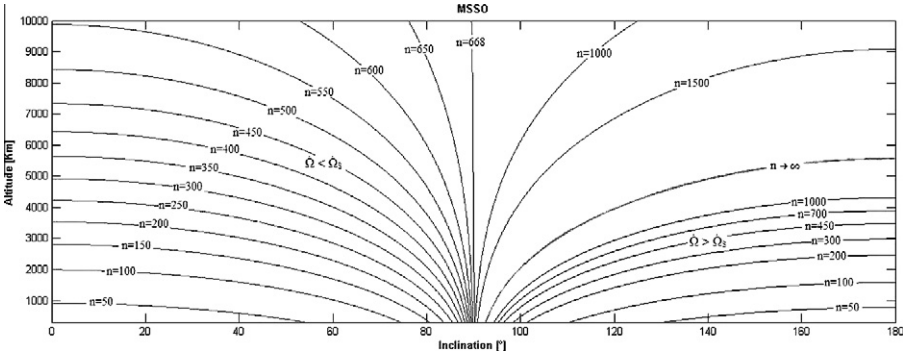

Fig. 7. Solution of Eq. (10) for Mars.

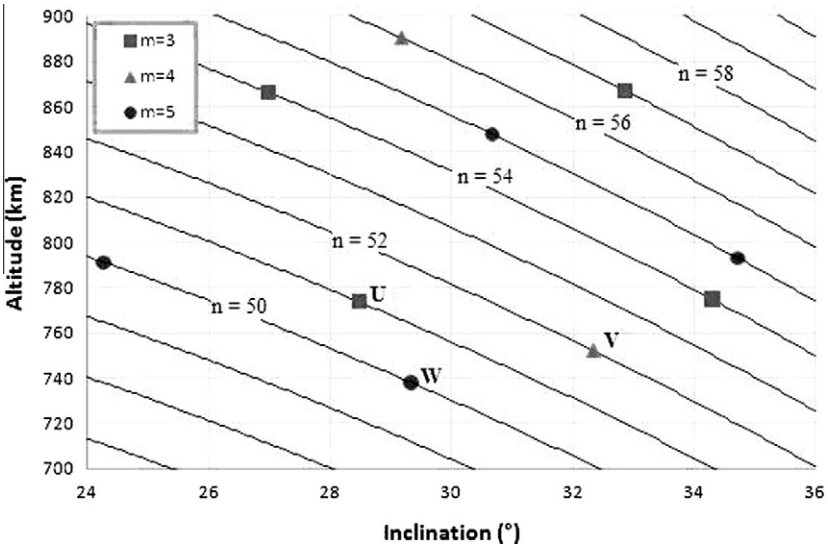

Fig. 8. Low and direct PMSSOs for the observation of low-latitudes of Mars.

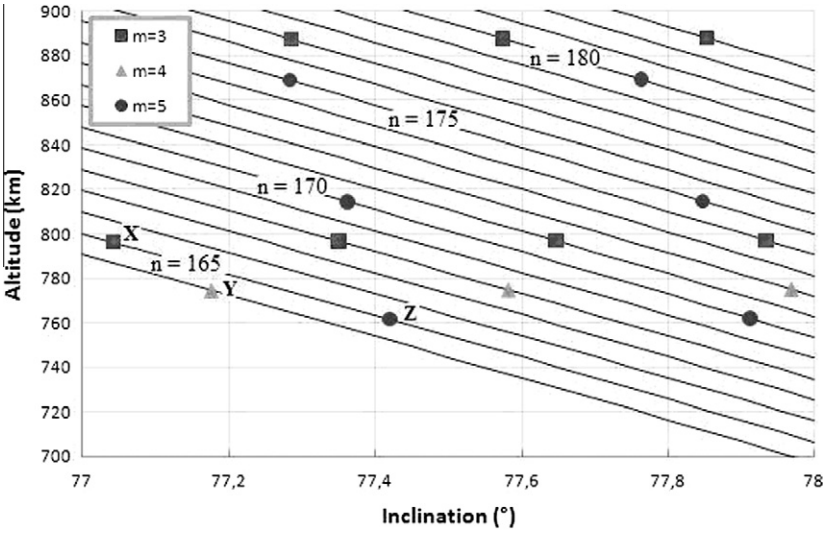

Fig. 9. Low and direct PMSSOs for the observation of high-latitudes of Mars.

Table 3
Parameters related to some PMSSO solutions reported in Figs. 8 and 9.

	m	n	k	N_t	q	h (km)	i (deg)	S_m (km)
U	3	51	2	32	10 + 2/3	773.75	28.47	667.99
V	4	52	3	43	10 + 3/4	752.01	32.34	497.10
W	5	50	4	54	10 + 4/5	738.12	29.32	395.85
X	3	165	2	32	10 + 2/3	796.38	77.04	667.98
Y	4	164	3	43	10 + 3/4	774.48	77.18	497.10
Z	5	165	4	54	10 + 4/5	761.62	77.42	395.84

("complete models" minus "Keplerian plus J_2") was computed. The value thus obtained is indicated as $\Delta\Omega$.

Fig. 10 shows the $\Delta\Omega$ as a function of i, for different values of h, for the Earth.

For example, considering $h = 700$ km and $i = 20°$, the difference in RAAN is approximately $-15°$ after 1 year (point P).

Similarly, Fig. 11 shows the $\Delta\Omega$ for Mars.

While for the Earth the $\Delta\Omega$ trend is monotonically increasing, for Mars there is an inversion in the RAAN variation trend. The necessity to take into account all planetary gravitational harmonics is especially important for $i < 60°$ and $i > 120°$, where the $\Delta\Omega$ is approximately double the $\Delta\Omega$ of the Earth. Note that for $i = 90°$ for the Earth,

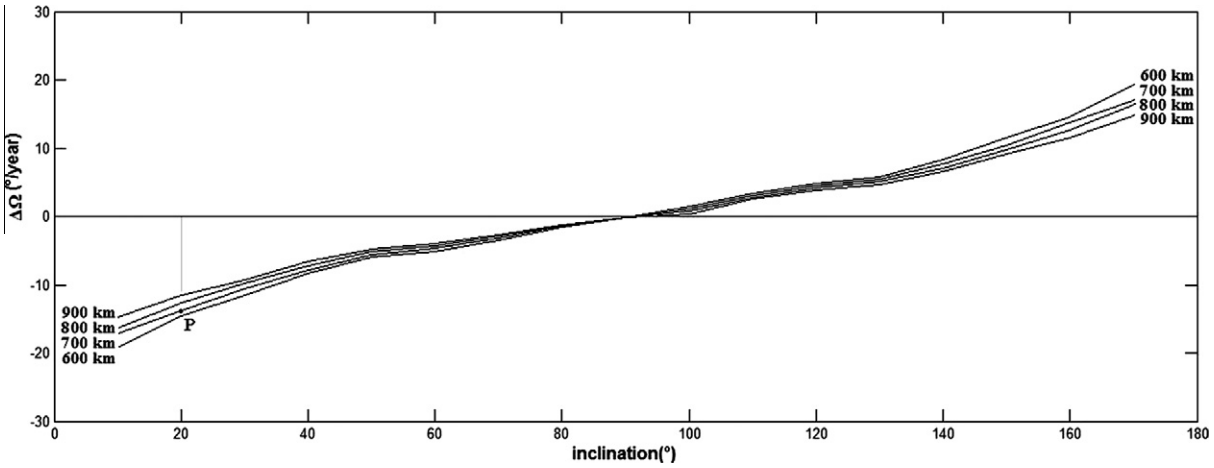

Fig. 10. $\Delta\Omega$ between the (21 × 21) and "Keplerian plus J_2" model for the Earth.

and for $i = 90°$ and approximately $90 \pm 22°$ for Mars, the $\Delta\Omega$ is null. The inversion in the $\Delta\Omega$ trend for Mars is mainly due to the first (4 × 4) harmonics of the gravitational field, which have an order of magnitude greater than the corresponding harmonics of the terrestrial gravitational field. A comparison between the models (4 × 4) and (40 × 40) showed a significant difference for $i < 30°$ and $i > 150°$ and therefore, for these values of inclination, it is necessary to take into consideration the (40 × 40) model.

It is evident that considering only the basic solution for the design is associated to an error; on the contrary, if the "complete" models are taken into account the error is negligible.

The trends obtained in Figs. 10 and 11 may be approximated by the following analytical expressions as a result of interpolations for data regarding the Earth (Eq. (19)) or Mars (Eq. (20)):

$$\Delta\Omega(r,i) \cong A_E(r) tg\left[\frac{3}{4}i + \frac{10\pi}{27}\right] \tag{19}$$

$$\Delta\Omega(r,i) \cong \alpha\left[A_M(r) + B_M(r)\cos\left(3i - \frac{\beta\pi}{3}\right)\right] \tag{20}$$

where in Eq. (20) $\alpha = -1$ and $\beta = 1$ for $i < 90°$, $\alpha = 1$ and $\beta = 2$ for $i \geqslant 90°$. Such relationships allow to determine the $\Delta\Omega$ value straightforwardly but their use may introduce a small error with respect to the cases obtained by numerical simulation in Figs. 10 and 11 (approximately 1°/year for the Earth and 2°/year for Mars).

Table 4 reports the values of the coefficients introduced in Eqs. (19) and (20).

The RAAN variation due to the superior harmonics of the gravitational field influences both the conditions of periodicity (1) and of Multi-SunSynchronism (2); in fact, the nodal day, which depends on the variation of RAAN through Eq. (4), is present both in (1) and in (2). Since the variation of RAAN due to gravitational perturbations of a planet depends, for a circular orbit, on the orbit altitude and inclination, the introduction of a corrective factor for the $\Delta\Omega$ leads to opportunely modify the orbit altitude

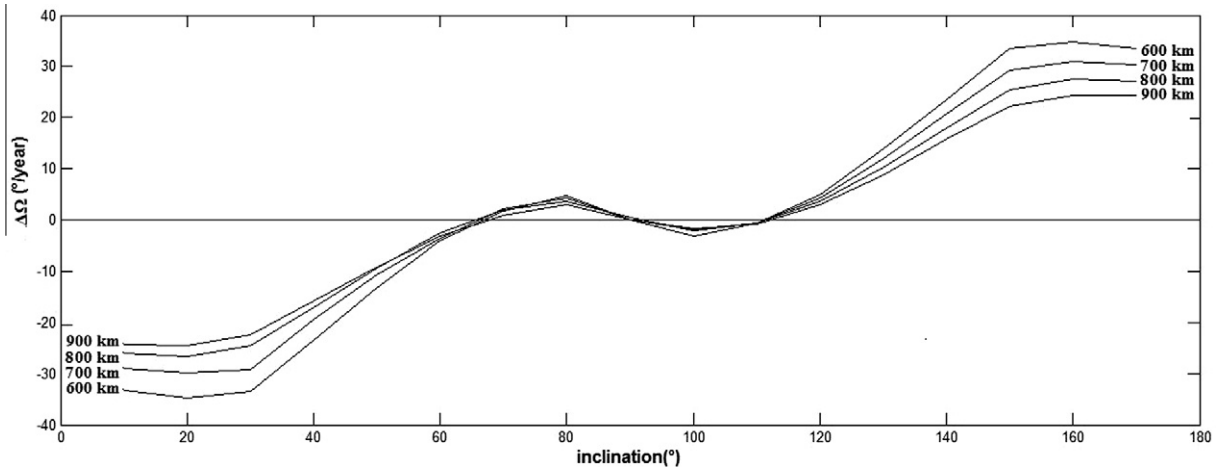

Fig. 11. $\Delta\Omega$ between the (40 × 40) and "Keplerian plus J_2" model for Mars.

Table 4
Coefficient of Eqs. (19) and (20) for $h = 600$, 700, 800, 900 km.

	$h = 600$ km	$h = 700$ km	$h = 800$ km	$h = 900$ km
A_E	11.0	10.1	9.4	8.9
A_M	15.0	13.0	11.6	10.7
B_M	19.5	17.3	15.4	13.5

Table 5
Difference between complete and basic solutions.

	h_{J2} (km)	$i = i_{J2}$ (deg)	$\Delta\Omega$ (deg/year)	Δh (km)
A (Earth)	700.58	26.09	−14.28	−12.67
U (Mars)	773.75	28.47	−27.14	−13.52
X (Mars)	796.38	77.04	2.87	5.81

and/or the inclination. Since it is possible to properly modify one of them, once the basic solution is retrieved by Eqs. (10) and (11), it is possible to obtain a precise PMSSO solution by applying a simple variation of the orbit altitude. In other words, the complete solution in terms of h may be represented by $h = h_{J2} + \Delta h$, where h_{J2} represents the basic solution and Δh the necessary variation of orbit altitude ($i = i_{J2}$).

If the additive factor Δh (corrective factor for the orbit altitude) of the complete solution is seen as a disturbing factor for the basic solution, in Eq. (6) it is possible to consider, in an approximate way, the sum of the variation of RAAN due to J_2 ($\Delta\Omega_{J2}$) and the one due to all the gravitational harmonics (disturbing term). By inverting such Eq. (6), it is possible to retrieve the necessary variation of orbit altitude:

$$\Delta h \cong \left(\frac{K_2 \cdot \cos i}{\Delta\Omega_{J2} + \Delta\Omega}\right)^{2/7} - (h_{J2} + R_P) \tag{21}$$

Table 5 shows the $\Delta\Omega$ for points A (in Fig. 5 and Table 1), U (in Fig. 8 and Table 3) and X (in Fig. 9 and Table 3) and the consequent difference of altitude Δh computed by Eq. (21).

As evidence shows, the introduction of a corrective factor, leaving the inclination steady, determines a variation of the orbit altitudes in the order of 5–10 km. Considering the corrective factor on the basic solution allows to avoid carrying out corrective manoeuvres out of plane in order to keep the RAAN value inside a certain tolerance depending on the accepted on-ground track shift; for example, in the case of point P in Fig. 10, the required annual velocity variation is equal to 1.96 km/s.

6. Conclusions

In this paper the feasibility of exploiting the use of the Periodic Multi-SunSynchronous Orbits has been investigated both for the observation of the Earth and of Mars taking into account single satellites and satellite constellations.

The Periodic Multi-SunSynchronous Orbits allow to obtain regular cycles of observation of a given area at different local times; therefore, they can be used profitably for all those remote sensing applications that may get advantage of data analysis deriving from measurements carried out on the same area but with different solar illumination conditions. Thus, unlike the classical PSSO, the use of the PMSSOs on Mars should allow an estimate of several atmospheric phenomena characterized by typical diurnal variations (cycle of the hazes and clouds, dynamics of the thermal tides, density variations, meteorology phenomena and water, CO_2, dust cycles, etc.).

The effects of the superior harmonics of the planetary gravitational field, more marked for Mars because of the more significant effects of the higher harmonics of the martian gravitational field, lead to the introduction of a corrective factor, depending on the orbital altitude and inclination. Such a corrective factor, which causes an appropriate setting of the initial value of the orbit altitude (which may differ of approximately 5–10 km from the one obtained considering only the oblateness of the planet), allows to avoid periodic corrective manoeuvres. Besides, simple analytical expressions causing an annual error of about 1° for the Earth and 2° for Mars was proposed. The use of a corrective factor on the basic solution allows to avoid corrective manoeuvres of the order of 2 km/s per year.

References

Bolle, A., Circi, C. Modified Sun-synchronous orbits by means of solar sails. Recent Patents on Space Technology 1 (1), 72–79, 2011.

Cantor, B., Malin, M., Edgett, K.S. Multiyear Mars orbiter camera (MOC) observations of repeated Martian weather phenomena during the northern summer season. Journal of Geophysical Research 107, 5014–5021, 2002.

Capderou, M., Forget, F. Optimal orbits for Mars atmosphere remote sensing. Planetary and Space Science 52, 789–798, 2004.

Goody, R., Belton, M.J.S. A discussion of Martian atmospheric dynamics. Planetary and Space Science 15 (2), 247–256, 1967.

Hess, S.L., Henry, R.M., Tillman, J.E. The seasonal variation of atmospheric pressure on Mars as affected by the south polar cap. Journal of Geophysical Research 84 (B6), 2923–2927, 1979.

Hopkins, R.G. Long-term revisit coverage using multi-satellite constellations, in: AIAA/AAS Astrodynamics Conference, Minneapolis, USA, AIAA Paper N. 88-4276-CP, 1988.

Kalil, F., Martikan, F. Derivation of nodal period of an Earth satellite and comparison of several first-order secular oblateness results. AIAA Journal 1 (9), 2041–2046, 1963.

Lemoine, F.G., Kenyon, S.C., Factor, J.K., Trimmer, R.G., Pavlis, N.K., Chinn, D.S., Cox, C.M., Klosko, S.M., Luthcke, S.B., Torrence, M.H., Wang, Y.M., Williamson, R.G., Pavlis, E.C., Rapp, R.H., Olson, T.R. The Development of the Joint NASA GSFC and NIMA Geopotential Model EGM96, NASA Goddard Space Flight Center, Greenbelt, Maryland, 20771 USA, July, 1998.

Lemoine, F.G., Smith, D.E., Rowlands, D.D., Zuber, M.T., Neumann, G.A., Chinn, D.S. An improved solution of the gravity field of Mars (GMM-2B) from Mars global surveyor. Journal of Geophysical Research 106 (E10), 23359–23376, 2001.

Paige, D.A., Wood, S.E. Modelling the Martian Seasonal CO_2 cycle 2. Interannual variability. Icarus 99 (1), 15–27, 1992.

Tamppari, L.K., Zurek, R.W., Paige, D.A. Viking-era diurnal Water–ice clouds. Journal of Geophysical Research 108, 1–9, 2003.

Ulivieri, C., Anselmo, L. Multi-Sun-Synchronous orbits for earth observation. Advances in the Astronautical Sciences, No. 76, Uninvelt Inc., San Diego, pp. 123–133, 1991.

Ulivieri, C., Castronuovo, M.M., Francioni, R., Cardillo, A. A split window algorithm for estimating land surface temperature from satellites. Advances in Space Research 14 (3), 59–65, 1994.